Real-Time Yield Point Prediction for Water-Based Drilling Mud using Particle Swarm Optimised Neural Network*

[1]S. Asante-Okyere and [1]H. Osei
[1]University of Mines and Technology, Tarkwa, Ghana.

Asante-Okyere S. and Osei H. (2024), "Real-Time Yield Point Prediction for Water-Based Drilling Mud using Particle Swarm Optimised Neural Network", *Ghana Mining Journal,* Vol. 24, No. 1, pp. 169-177.

Abstract

Yield point (YP) is an essential rheological property of drilling mud that influences the ability of the mud to lift well cuttings from the annulus to the surface, impacting the overall drilling efficiency. Despite its significance, YP is typically measured only once or twice a day using complex rheometers. On the other hand, a simple field equipment such as the Marsh funnel is used to constantly monitor the drilling fluid's behaviour up to about 144 times daily. This only provides an indication of the drilling fluid condition and not detailed rheological characteristics. There have been previous attempts to infer the rheological characteristics from the constantly monitored Marsh funnel parameters. One of the widely used approach to estimate rheological properties from Marsh funnel parameters has been the implementation of Back Propagation Neural Network (BPNN). BPNN algorithm exhibits some drawbacks such as poor generalisation. Based on that, the present study improved the performance of BPNN in predicting YP using particle swarm optimsation (PSO) based BPNN. It was identified from the study that PSO-BPNN outperformed BPNN in the estimation of YP in terms of correlation coefficient (R) and mean square error (MSE) and variance accounted for (VAF). During testing PSO-BPNN attained 0.929, 1.129 and 92.29 % as *R, MSE* and *VAF* score, respectively, while *BPNN* had 0.868, 1.235 and 83.78 % for *R, MSE* and *VAF* score, respectively. These findings suggest that *PSO-BPNN* offers a more reliable and efficient approach to predicting drilling fluid yield point from Marsh funnel experimentation.

Keywords: Drilling fluid, yield point, particle swarm optimisation, artificial neural network, mud density, Marsh funnel viscosity.

1 Introduction

Drilling fluids are essential in drilling operations, facilitating various processes such as wellbore cleaning and pressure control. The three primary categories of drilling fluids include water-based mud, oil-based mud, and synthetic-based mud, each optimised for specific downhole conditions of pressure and temperature to improve drilling performance. The primary function of drilling fluids is to clean the wellbore by transporting drilled cuttings from the bottom of the hole to the surface. Once the cuttings reach the surface, they are processed by solid control equipment to separate them from the fluid. The cleaned and reconditioned fluid is then recirculated back into the well to continue the drilling operation efficiently.

Yield Point (YP) is a critical rheological property of drilling mud that measures the fluid's resistance to initial flow and provides insight into the attractive forces among the solids in the mud. The *YP* depicts the capacity of the drilling mud to lift well cuttings from the annulus to the surface. It is a good indicator of the antiparticle attraction of the solids in the drilling fluid and it can be controlled by additives such as chemical thinners, dispersants and viscosifiers (Adams, 1985) . In the field, *YP* is calculated as the difference between the 300-rpm dial reading of a rheometer and the Plastic Viscosity (PV) of the drilling mud. These measurements are commonly made using multi-speed rotational or capillary rheometers, with rotational rheometers featuring coaxial cylinders being the most frequently used. It was discovered by Luo *et al.* (1994) that turbulent flow conditions require lower *YP* of drilling mud to achieve a higher lifting force whereas a high *YP* of drilling mud is desirable in laminar flow conditions for high fluid drag force aiding cutting removal. It was further observed that it is more effective to regulate the *YP* than plastic viscosity to inhibit hole cleaning issues. Increasing *YP/PV* ratio in laminar flow will elevate the hole cleaning efficiency (Elkatatny *et al.*, 2016). Therefore, *YP*, *PV*, and Apparent Viscosity (AV) are important factors in evaluating drilling fluid performance, particularly for cleaning the wellbore. These rheological properties of *YP*, *PV* and *AV* are typically measured once or twice a day (Elkatatny *et al.*, 2016).

Due to the limitations of performing comprehensive rheological measurements frequently, parameters such as Marsh funnel viscosity, solid content, and drilling fluid density are monitored more frequently, every 10 to 15 minutes, using simpler field instruments in the form of Marsh funnel. The Marsh funnel is an inexpensive and quick tool that can

*Manuscript received February 02, 2024
Revised version accepted July 25, 2024
https://doi.org/10.4314/gm.v22i1.3

provide insights into the fluid's behaviour by measuring the time it takes for a specific volume of fluid to flow through the funnel. This frequent monitoring provides a more continuous assessment of the drilling fluid's condition, allowing for timely adjustments to maintain optimal performance. However, it is important to note that Marsh funnel parameters can only give an indication of the drilling fluid condition and not detailed rheological characteristics.

During the drilling operation, there is a pressing need for regular monitoring of parameters like *YP*, *PV*, and *AV* to ensure that the drilling fluid maintains its effectiveness in carrying cuttings to the surface.

1.1 Review of Previous Studies

Several studies have focused on predicting the viscosity of drilling fluid using simple, field-measurable parameters like Marsh funnel viscosity and mud density.

Pitt (2000) developed a correlation to convert Marsh funnel viscosity to the effective viscosity of drilling fluids as a function of drainage time and mud weight based on Eq. (1)

$$AV = D(T - 25) \quad (1)$$

where *AV* is apparent viscosity, *D* is fluid density and *T* is Marsh funnel time

Building on this work, Almahdawi *et al*. (2014) introduced a new model to estimate the apparent viscosity of drilling fluids based on Marsh funnel viscosity and fluid density. Their research concluded that their proposed equation provided more accurate results than Pitt's model as expressed in Eq. (2).

$$AV = \left(-0.0118 \times T^2\right) + \left(1.6175T\right) - 32.168 \quad (2)$$

Almahdawi *et al*. (2016) further suggested that using a constant of 28 instead of 25, as used by Pitt (2000), yielded better results.

With the benefits of Artificial Intelligence (AI) over the mathematical modelling approach, Elkatany *et al.* (2016) first developed an artificial neural network (ANN) model for predicting the rheological properties of drilling fluid from Marsh funnel viscosity, solid content and density values in real-time using back propagation neural network (*BPNN*) algorithm.
Furthermore, Marsh funnel viscosity and solid percent were used as input variables to develop a *BPNN* model for providing real-time rheological properties of KCl-water based drilling fluid (Elkatany, 2017). By converting the *BPNN* "black box" into a "white box," Elkatany (2017) was able to extract mathematical models that predict rheological parameters. The average absolute error for all correlations was less than 6 %, and the correlation coefficient was greater than 90 %. These developed correlations provide high accuracy in predicting drilling fluid properties, eliminating the need for labor-intensive laboratory measurements and allowing for real-time property assessment.

Gowda *et al*. (2020) also developed a rheological parameter estimator for high-bentonite drilling mud using Marsh funnel parameter based on BPNN. High-bentonite mud (HBM) is a water-based drilling fluid known for its enhanced cutting removal and hole cleaning efficiency. Periodic monitoring of the rheological properties of HBM is essential for optimizing drilling operations. The *BPNN* models showed a significant match between the predicted and measured rheological properties, with a high correlation coefficient (*R*) above 0.90 and a maximum average absolute percentage error (AAPE) of 6%.

1.2 Enhancing BPNN Performance with Particle Swarm Optimization

From the literature reviewed, the *BPNN* is widely used to predict the rheological properties of drilling fluids from Marsh funnel parameters. However, *BPNN* has notable shortcomings, including poor generalisation performance due to overfitting and slow convergence during training.

Swarm intelligence algorithms, such as Particle Swarm Optimisation (PSO), offer a solution to these limitations. PSO improves the performance of BPNN by effectively exploring the search space to find the global optimum with minimal human intervention. This optimisation leads to better generalization and faster convergence, enhancing the neural network's predictive capabilities. This was evidently seen when PSO outperformed other optimisers in predicting PV and AV in the study of Youcefi *et al.* (2021).

The objective of this study is to enhance the performance of BPNN in estimating the viscosity of water-based drilling mud from Marsh funnel experimental data using the PSO algorithm. By integrating PSO with BPNN, the study aims to develop a more robust and accurate model for predicting drilling fluid properties in real time, thereby improving operational efficiency and decision-making during drilling processes.

2 Resources and Methods Used

2.1 Data

Data used for the present study was obtained from an exploratory well located in the North Sea. The data constituted measured depth in meters, mud weight in g/cm^3, Marsh funnel viscosity in mPa.s

and *YP* in Pa.s. The data description used for the development of the models is summarised in Table 1 and graphically represented in Figs. 2 and 3. This study employed 69 data points with 80 % of the data randomly selected for training and 20 % for testing. In addition, MATLAB 2021a was used to develop the neural network models.

Table 1 Data Description

Type of Data	Minimum	Maximum	Average
Depth (m)	651	3 574	3 061
Viscosity (mPa.s)	6.00	62.00	17.74
Mud Weight (g/cm^3)	1.05	1.64	1.54
Yield Point (Pa)	1.90	16.30	6.69

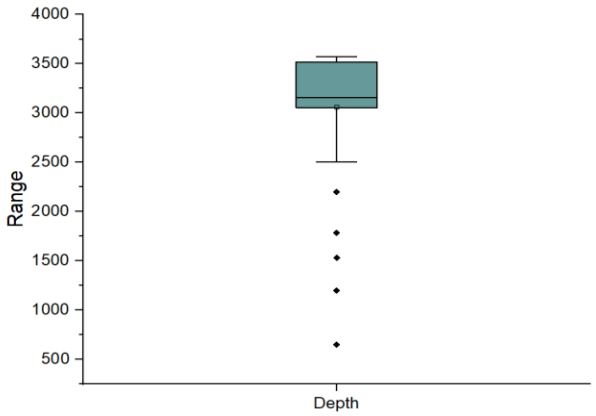

Fig. 1 Boxplot for depth as an input variable

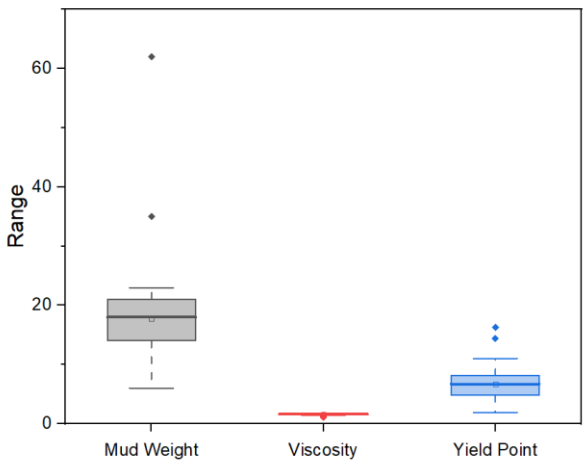

Fig. 2 Boxplot for mud weight, viscosity and YP as input variables

2.2 Data Normalisation

As a result of the difficulty of the training process and the decline in network performance without normalisation, data must be normalised before it can be used for training. The objective of data normalisation is to demonstrate that the statistical distribution of values for each net input and output is relatively stable. Additionally, the values must be adjusted to align with the input neuron range (Razi *et al.*, 2013). The input data was normalised within a range of -1 and 1. This is shown in Eq. (1).

$$I = I_{min} + (I_{max} - I_{min})\ x\ \frac{(D - D_{min})}{(D_{max} - D_{min})} \qquad (1)$$

where, I = normalised data
D = measured values
D_{min} = minimum measured value
D_{max} = maximum measured value
I_{max} and I_{min} values are set at 1 and -1.

2.3 Back Propagation Neural Network

Back propagation neural networks (BPNNs) are a popular choice for supervised neural networks due to their straightforward implementation and efficient gradient descent computation. The *BPNN* algorithm involves forward propagation of input data and backward propagation of output error (Bullinaria, 2004). The primary goal of *BPNN* is to optimise the network's weights to minimize the error margin. The mathematical formula for determining the optimal weights is presented in Eq. (2) (Konaté *et al.*, 2015).

$$W^* = \arg\min E_p(w) \qquad (2)$$

where w is weight matrix and $Ep(w)$ is an objective function on w.

$E(w)$ is the error that is to be reduced at any point of w as seen in Eq. (3) (Konate´ *et al.*, 2015; Asante-Okyere *et al.*, 2018).

$$E(w) = \sum_p E_p(w) \qquad (3)$$

where p is the number of training samples and the error for each sample well log point is given as $Ep(w)$ as represented in Eq. (4) (Konate´ *et al.*, 2015; Asante-Okyere *et al.*, 2018).

$$E_p = \frac{1}{2}\sum_p \left(d_{pj} - y_{pj}(w)\right)^2 \qquad (4)$$

2.4 Training Process of *BPNN*

Training is the process of appropriating connection weights. The majority of training procedures

commence by assigning random numbers to the matrix of weights. The authenticity of the network is further evaluated. Also, the weights are modified based on the performance validity of the neural network (Razi *et al.*, 2013). The neural network was trained using the Levenberg-Marquardt backpropagation technique. The maximum number of iteration used was 1000. A sequential trial and error method was implemented to obtain the optimal *BPNN* model structure by adjusting the number of hidden neurons. Fig. 1 depicts a flow chart of the *BPNN* procedure.

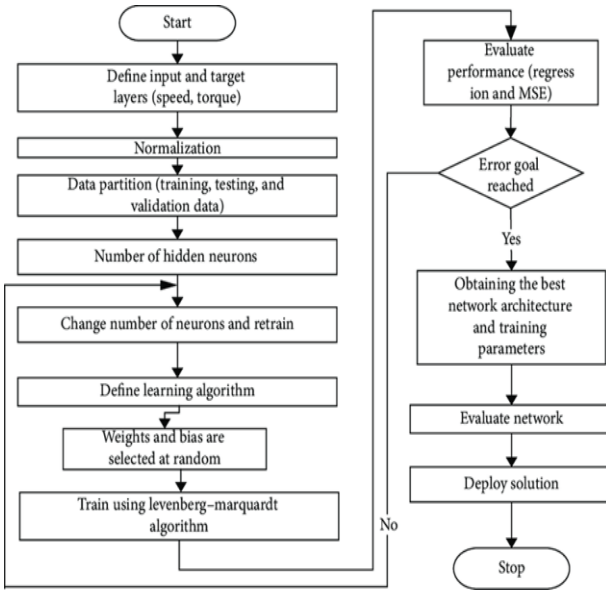

Fig. 3 Flow Chart of ANN (Source: Tariq et al., 2020)

2.5 Particle Swarm Optimisation

The modelling of social behaviour is what drives particle swarm optimisation. By using an operator in accordance with the fitness information gathered from the environment, this optimisation strategy updates the population of individuals, causing the population as a whole to migrate towards better solution regions (Illias *et al.*, 2015). Fig. 2 depicts a flow chart of PSO procedure.

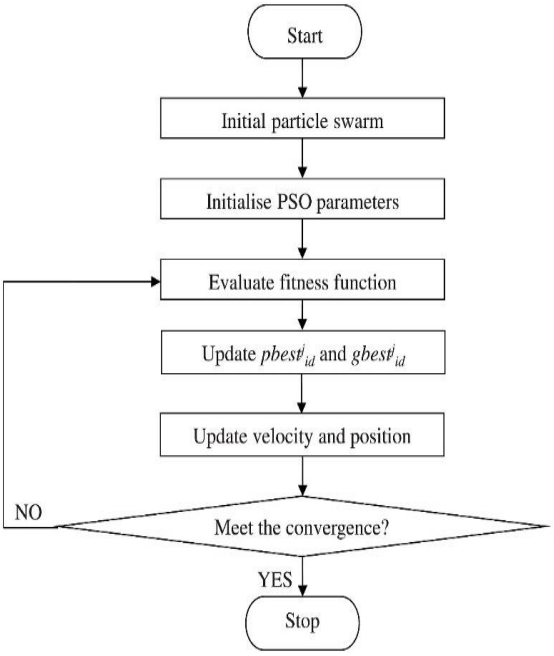

Fig. 4 Flow Chart of PSO (Source: Illias et al., 2015)

2.5.1 Problem Definition

The problem is formulated into a form known as the objective or cost function. The objective is to minimise the value of the cost function. In this section, the number of unknown variables or decision variables are specified. Additionally, a definition of the decision matrix is also provided with the upper and lower bounds determined by the range of the decision variables.

2.5.2 Parameters of Particle Swarm Optimisation

The specification of the swarm size or population size is followed by the highest number of iterations for the particle swarm. A large swarm makes it possible to expand the area covered per iteration in the solution space. If a suitable uniform initialisation approach is used to initialise the particles, the greater the swarming particles, the higher the initial heterogeneity of the swarm. The learning coefficient, one of the remaining characteristics to be determined and additionally provided, is the inertia weight. The parameters C_1 and C_2, which indicate a particle's certainty in itself and in its surroundings, respectively, are also regarded as the acceleration metrics. The inertia weight is the key determinant in the PSO's convergence behaviour. High inertia weight causes the optimisation to converge more slowly, whereas low inertia weight causes local entrapment (Maurya *et al.*, 2019). The maximum population size was 300.

2.5.3 Initialisation of Particle Swarm Optimisation

Particle initialisation has an essential role in the performance of PSO. If the initialisation is poor, the

algorithm may search in undesirable areas, making it difficult to find the optimal solution. Performance of PSO is highly dependent on the initialisation of swarms (Imran *et al.*, 2013). All initialisation procedures required to launch the particle swarm optimisation are implemented in this section. As part of this, population arrays are created, particle positions are initialised, evaluated and initial best values for the global and personal also initialised. Global best uses a position-velocity update approach to examine a set of potential solutions and seek to identify the optimal one. Personal best is comparable to global best but because it has a ring topology, the particles are drawn to the area around it. A variety of structures are used to store information and the data of swarming particles.

2.5.3 Main Loop of Particle Swarm Optimisation

The primary loop used in particle swarm optimisation is a loop that runs from the first iteration up to the specified maximum number of iterations. The position and speed of every particle is analysed and updated after each iteration. The maximum iteration used for the model is 1 000.

2.6 Statistical Parameters

The performance of the drilling fluid *YP* prediction model from *PSO-BPNN* and *BPNN* was determined using statistical parameters namely correlation coefficient (*R*), mean square error (*MSE*) and variance accounted for (*VAF*). The correlation between the prediction from the models and measured *YP* was explained by the *R* value (Eq. 5). The *R* value ranges from 0 to 1, with a strong correlation existing if the *R* value approaches 1. The average square deviation between the observed and predicted yield point values were also expressed using the *MSE* value shown in Eq. (6). The *MSE* value provides an indication of how much the estimates deviate from the measured density log data and reflects the quality of the predictive model. The *VAF* shows the degree of the variance of the measured data captured by the prediction.

$$R = \frac{\sum_{i=1}^{n}\left(m_i - \overline{m}\right)\left(g_i - \overline{g}\right)}{\sqrt{\sum_{i=1}^{n}\left(g_i - \overline{g}\right)^2}\sqrt{\sum_{i=1}^{n}\left(m_i - \overline{m}\right)^2}} \quad (5)$$

$$MSE = \frac{1}{n}\sum_{i=1}^{n}\left(m_i - g_i\right)^2 \quad (6)$$

$$VAF = \left(1 - \frac{\sum_{i=1}^{n}\left(m_i - \overline{m}\right)^2}{\sum_{i=1}^{n}\left(m_i - g_i\right)^2}\right) \times 100\% \quad (7)$$

where *g* is the predicted drilling fluid *YP*, *m* is the measured *YP* and *n* is the total number of observations.

3 Results and Discussion

3.1 BPNN model structure

After a sequential trial and error method, eight hidden neurons were optimum for the *BPNN* model as indicated in Table 2. This implies that at a model structure of three inputs, a hidden layer with eight hidden neurons and one output layer, the highest correlation coefficient and lowest mean squared error values were obtained. Fig.s 3 and 4 show the correlation plot for the training and testing stages respectively. During training, the correlation coefficient varied across different neuron counts, indicating variations in the model's performance. As indicated in Table 2, the optimal *BPNN* obtained an *R* value of 0.86867 when training and 0.86836 during testing.

Table 2 Optimal BPNN structure

Number of hidden neurons	Training correlation coefficient (R)	Testing correlation coefficient (R)
1	0.01336	0.00869
2	0.56600	0.67502
3	0.54660	0.34767
4	0.83566	0.67744
5	0.69277	0.6974
6	0.85780	0.56422
7	0.58861	0.43189
8	**0.86867**	**0.86836**
9	0.47568	0.65718
10	0.20220	0.79882
11	0.90217	0.64646
12	0.74397	0.47267
13	0.90637	0.18280
14	0.67594	0.82671
15	0.82280	0.43786
16	0.58823	0.40919
17	0.5553	0.21673
18	0.53125	0.88741
19	0.83491	0.68633

20	0.79150	0.68603
21	0.81161	0.76245
22	0.89326	0.85755
23	0.51409	0.52721
24	0.87446	0.5809
25	0.44871	0.079289
⋮	⋮	⋮
100	0.44278	0.70893

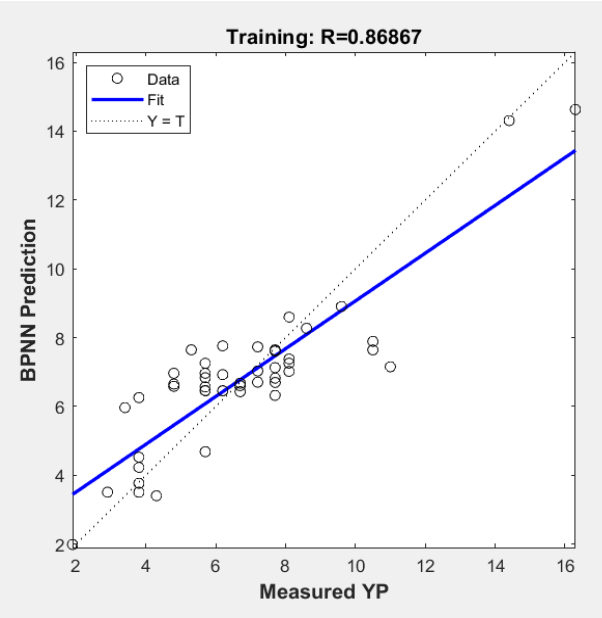

Fig. 5 Training Correlation Plot for the Optimal BPNN Model

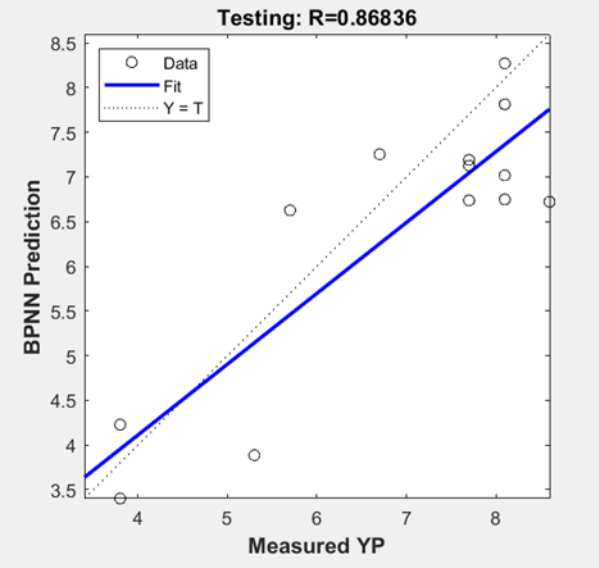

Fig. 6 Testing Correlation Plot for the Optimal BPNN Model

3.2 PSO-BPNN Model Structure

In order to enhance the performance of the *BPNN* model, *PSO* was employed to further improve the *BPNN* results by selecting the optimal weights and biases for the model.

The correlation plot for the training and testing samples is depicted in Fig.s 7 and 8 respectively. Table 3 shows the *PSO-BPNN* parameters used. The optimal *PSO-BPNN YP* model had a training and testing correlation coefficient of 0.90721 and 0.92885 respectively (Figs. 7 and 8).

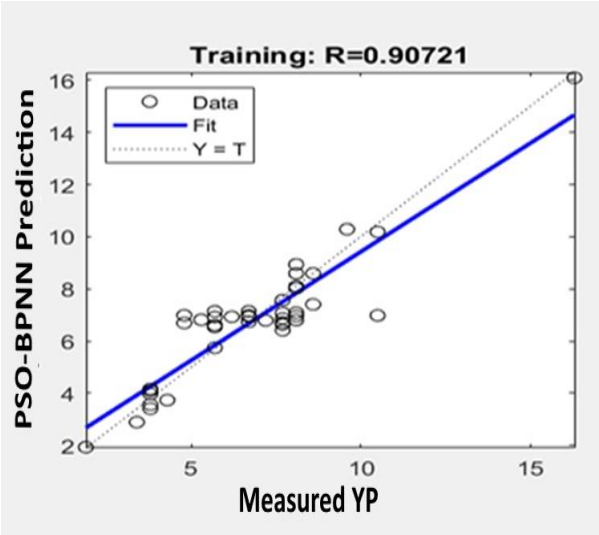

Fig. 7 Training Correlation Plot for PSO- BPNN

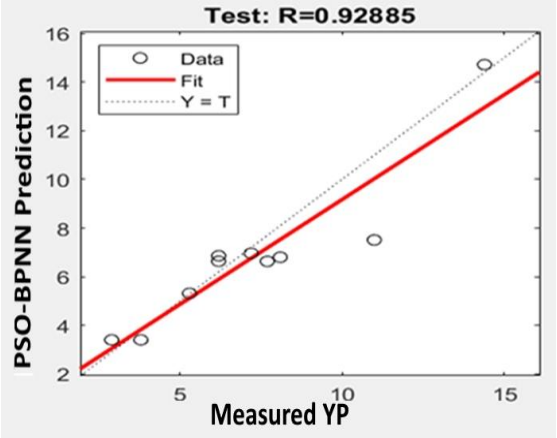

Fig. 8 Testing Correlation Plot for PSO- BPNN

Table 3 PSO-ANN Parameters

Parameter	Value
Population Size	300
Upper Bound	5
Lower Bound	-5
Maximum Iteration	1000
Cognitive Constant (C_1)	1.5
Social Constant (C_2)	2.5

3.3 Discussion

The training results presented in Table 3 indicate a comparative analysis of the performance of *BPNN* and *PSO-BPNN* in predicting the *YP* of drilling fluid. The *PSO-BPNN* model achieved an *R* value of 0.90721, significantly higher than the *BPNN*'s R value of 0.86867. This indicates that the *PSO-BPNN* model has a stronger ability to capture the underlying patterns in the training data compared to the *BPNN*. A higher *R* value suggests that the training predictions from the *PSO-BPNN* model are more closely aligned with the actual values, demonstrating improvement in the *BPNN*s performance.

The *PSO-BPNN* model recorded an *MSE* of 1.0160, which is lower than the *BPNN*'s *MSE* of 1.2326 as indicated in Table 3. A lower *MSE* value signifies that the training predictions made by the *PSO-BPNN* model are more accurate, with smaller deviations from the actual values. This reduction in error highlights the effectiveness of the *PSO* algorithm in optimizing the neural network, resulting in more precise predictions.

The *PSO-BPNN* model achieved a *VAF* of 0.900798 or 90.0798 %, higher than the *BPNN*'s *VAF* of 0.838089 or 83.8089 % (Table 3). A higher variance indicates that the model can explain a greater proportion of the variability in the training data. This suggests that the *PSO-BPNN* model has better captured the complexity and variability of the training data.

During the testing stage, the PSO-*BPNN* model achieved a correlation coefficient of 0.92885, indicating a stronger correlation between predicted and actual values compared to the *BPNN* model, which had an *R* value of 0.86836 as summarised in Table 4. This significant improvement suggests that the *PSO-BPNN* model provides more accurate predictions, effectively capturing the relationship between input variables of Marsh funnel parameters and the *YP* of drilling fluid.

When evaluating prediction errors, the *PSO-BPNN* model demonstrated a lower mean squared error (*MSE*) of 1.1287, as opposed to the *BPNN* model's *MSE* of 1.2350 (Table 4). This reduction in *MSE* indicates that the *PSO-BPNN* model's predictions are closer to the actual values, reflecting fewer deviations and better overall accuracy in its predictive performance.

The *PSO-BPNN* model also showed a higher variance (*VAF*) of 0.92285 or 92.285 % compared to the BPNN model's *VAF* of 0.83779 or 83.779 % (Table 4). This increased variance signifies that the *PSO-BPNN* model explains a larger portion of the variability in the testing data, indicating a more comprehensive and reliable understanding of the data's underlying patterns.

Table 3 Comparing the training performance of PSO-BPNN and BPNN in predicting YP of drilling fluid

Indicator	BPNN	PSO-BPNN
R	0.86867	0.90721
MSE	1.2326	1.016
VAF	0.838089	0.900798

Table 4 Comparing the testing performance of PSO-BPNN and BPNN in predicting YP of drilling fluid

Indicator	BPNN	PSO-BPNN
R	0.86836	0.92885
MSE	1.2350	1.1287
VAF	0.83779	0.92285

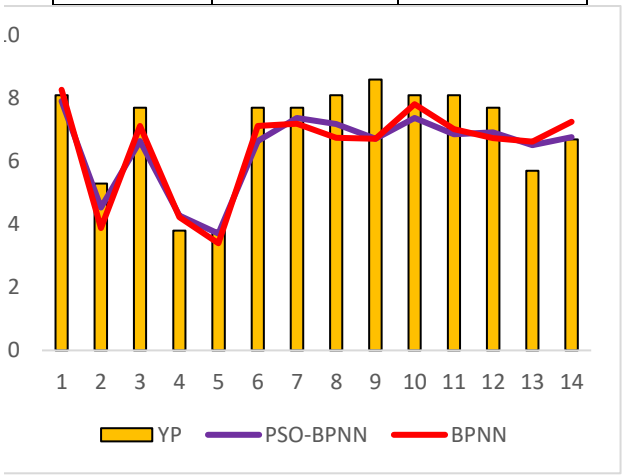

Fig. 9 YP Prediction performance of PSO-BPNN and BPNN

4 Conclusions

This study aimed to enhance the prediction of *YP* from Marsh funnel data by integrating *PSO* with a *BPNN*. The performance of the *PSO-BPNN* model was compared with the traditional *BPNN* model using data from an exploratory well in the North Sea. During training, the *PSO-BPNN* model demonstrated superior performance with a higher correlation coefficient (R = 0.90721) and lower mean squared error (*MSE* = 1.016) compared to the *BPNN* model (R = 0.86867, *MSE* = 1.2326). The *PSO-BPNN* model also exhibited a higher variance accounted for (*VAF* = 90.08%) than the *BPNN* model (*VAF* = 83.81%). Testing results further confirmed the superiority of the *PSO-BPNN* model, achieving a testing correlation coefficient of 0.92885, significantly higher than the *BPNN* model's 0.86836. Additionally, the *PSO-BPNN* model recorded a lower *MSE* (1.1287) compared to the *BPNN* model (1.2350) and a higher *VAF* (92.29%) than the *BPNN* model (83.78%). These findings indicate that the *PSO-BPNN* model provides a more reliable and efficient approach to predicting the *YP* of drilling fluids from Marsh funnel data. The enhanced performance suggests its potential application for real-time drilling fluid management and optimization, contributing to more effective and efficient drilling operations.

References

Adams, N. J. (1985), *Drilling engineering : A Complete Well Planning Approach*, PennWell Books, Tulsa, 227 pp.

Akinnikawe, O., Lyne, S. and Roberts, J. (2018), "Synthetic Well Log Generation using Machine Learning Techniques", *SPE/AAPG/SEG Unconventional Resources Technology Conference*, Houston, Texas, USA, pp. 1-16.

Almahdawi, F. H., Al-Yaseri, A. Z., and Jasim, N. (2014), "Apparent Viscosity Direct from Marsh Funnel Test", *Iraqi Journal of Chemical and Petroleum Engineering*, Vol. 15, No. 1, pp. 51-57.

Al-Azani, K., Elkatatny, S., Abdulraheem, A., Mahmoud, M., and Al-Shehri, D. (2018), "Real Time Prediction of the Rheological Properties of Oil-based Drilling Fluids using Artificial Neural Networks", In *SPE Kingdom of Saudi Arabia annual technical symposium and exhibition*, pp. SPE-192199.

Asante-Okyere, S., Xu, Q., Mensah, R. A., Jin, C. and Ziggah, Y. Y. (2018), "Generalized Regression and Feed Forward Back Propagation Neural Networks in Modelling Flammability Characteristics of Polymethyl Methacrylate (PMMA)", *Thermochimica Acta*, Vol. 667, pp. 79–92.

Bullinaria, J. A. (2004) "Introduction to Neural Networks", *Unpublished MSc Lecture Notes*, University of Birmingham, UK, pp. 1-16.

Elkatatny, S., Tariq, Z. and Mahmoud, M. (2016), "Real Time Prediction Of Drilling Fluid Rheological Properties Using Artificial Neural Networks Visible Mathematical Model", *Journal of Petroleum Science and Engineering*, Vol. 146, pp. 1202 – 1210.

Elkatatny, S. (2017), "Real-time prediction of rheological parameters of KCL water-based drilling fluid using artificial neural networks" *Arabian Journal for Science and Engineering*, Vol. 42, pp. 1655-1665.

Gowda, A., Elkatatny, S., Abdelgawad, K., and Gajbhiye, R. (2020), "Newly Developed Correlations to Predict the Rheological Parameters of High-Bentonite Drilling Fluid using Neural Networks", *Sensors*, Vol. 20, No. 10, pp. 2787.

Illias, H. A., Chai, X. R., Mokhlis, H. and Abu Bakar, A. H. (2015), "Transformer Incipient Fault Prediction Using Combined Artificial Neural Network and Various Particle Swarm Optimisation Techniques", *PLoS ONE*, pp.1 – 5.

Imran, M., Hashim, R. and Khalid, N. E. A. (2013), "An Overview Of Particle Swarm Optimization Variants", *Procedia Engineering*, pp. 491 – 496.

Konate´, A. A., Pan, H., Khan, N. and Yang, J. H. (2015), "Generalized Regression and Feed-Forward Back Propagation Neural Networks in Modelling Porosity from Geophysical Well Logs", *J. Petrol Explor. Prod. Technol.*, Vol. 5, No. 2, pp. 157–166.

Luo, Y., Bern, P. A., Chambers, B. D. and Kellingray, D. S. (1994), "Charts Determine Hole Cleaning Requirements in Deviated Wells", *Oil and Gas Journal*, pp. 499 – 505

Maurya, H., Bohra, V. K., Pal, N. S. and Bhadoria, V. S. (2019), "Effect of Inertia Weight of PSO on Optimal Placement of DG", *IOP Conference Series: Materials Science and Engineering*, Vol. 594, No. 1, pp. 1 - 12.

Pitt, M. J. (2000), "The Marsh funnel and Drilling Fluid Viscosity: A New Equation for Field Use", *SPE Drilling & Completion*, Vol. *15* No. 01, pp. 3-6.

Razi, M. M., Mazidi, M., Razi, F. M., Aligolzadeh, H. and Niazi, S. (2013), "Artificial Neural Network Modeling of Plastic Viscosity, Yield Point and Apparent Viscosity for Water-Based Drilling Fluids", *Journal of Dispersion Science and Technology*, Vol. 34, No. 6, pp. 822 – 827.

Tariq, I., Muzzammel, R., Alqasmi, U. and Raza, A. (2020), "Artificial Neural Network-Based Control of Switched Reluctance Motor for Torque Ripple Reduction", *Mathematical Problems in Engineering*, Vol. 2, pp. 1 – 5.

Youcefi, M. R., Hadjadj, A., Bentriou, A., & Boukredera, F. S. (2022), "Real-Time Prediction of Plastic Viscosity and Apparent Viscosity for Oil-Based Drilling Fluids Using a Committee Machine with Intelligent Systems", *Arabian Journal for Science and Engineering*, pp. 1-14.

Authors

S. Asante-Okyere is currently a Lecturer in the Department of Petroleum and Natural Gas Engineering, Univerisity of Mines and Technology. He holds a PhD and MEng in Oil and Natural Gas Engineering from the China University of Geosciences, China and BSc from the Kwame Nkrumah University of Science and Technology, Ghana. He is a member of the Society of Petroleum Engineers (SPE), American Association of Petroleum Geologists (AAPG), International Association of Mathematical Geosciences (IAMG) and other professional organizations. His research interest is in the application of artificial intelligence for petrophysical analysis, reservoir characterization and source rock geochemistry.

H. Osei is currently a senior lecturer at the Department of Petroleum and Natural Gas Enginering of the University of Mines and Technology, Tarkwa, Ghana. He holds MSc degree in Petroleum Engineering from African University of Science and Technology, Abuja, Nigeria. He obtained his PhD degree in Mechanical Engineering from the Universiti Teknologi PETRONAS (UTP), Perak, Malaysia. He is a member of Society of Petroleum Engineers, International Association of Engineers, Universal Association of Mechanical and Aeronautical Engineers, Teaching and Education Research Association and Ghana Institution of Engineering and Technology. His research interests include reservoir and production engineering, multiphase flow, fluid dynamics and separations technology.